Modeling salt-fingering structures

by Otto Zeman[1] and John L. Lumley[2]

ABSTRACT

Results are presented of calculations with a second-order turbulence model which has been modified to evolve continuously from full turbulent convection to thermo-haline convection, under appropriate circumstances. A three-layer system is simulated, with a salt-fingering interface between two convectively-driven turbulent layers. Experimental results on the salt/heat flux ratio are reproduced.

1. Introduction

Salt fingering belongs to a class of phenomena called double-diffusive convection (Turner, 1974). Salt fingering may occur at the interface of a warm, salty layer of water overlying a cooler, less salty layer. The saltier water stays on top because its higher temperature more than compensates for the top-heavy distribution of salt, and the overall density stratification is stable if molecular diffusion is neglected. If the interface is disturbed, the difference between the molecular diffusivities of salt and heat lead to a double-diffusive convective instability (Stern, 1960) manifested by columns of rising (cold) and sinking (hot) water which approximately retain the salt content of their initial elevation; motion in these columns is almost vertical with an overall finger-like appearance. These salt-fingering structures have been generated in the laboratory (Turner, 1967; Linden, 1973; Griffiths and Ruddick, 1980) and gained acceptance as a naturally occurring phenomenon, for example, on the underside of the Mediterranean outflow (Williams, 1975). Excellent reviews of this type of phenomenon are Turner (1974) and Sherman *et al.* (1978).

There is mounting observational evidence of salt fingering and its importance in mixing (very efficiently) salt and heat across density interfaces in the oceans. A lucid account of the history of research on and the search for salt fingers is in Kerr (1981).

The modeling effort lags behind the experiments. The stumbling block in successful modeling is that a salt-fingering interface (hereafter SFI) cannot be modeled in

1. Chesapeake Bay Institute, The Johns Hopkins University, Baltimore, Maryland, 21218, U.S.A.
2. Sibley School of Mechanical and Aerospace Engineering, Cornell University, Ithaca, New York, 14853, U.S.A.

isolation from its environment. The positive buoyant flux through the SFI causes convective instability, maintaining fairly deep turbulent convective regions between two neighboring SFI's. Hence the simplest autonomous salt-fingering structure consists of one SFI sandwiched between two convective layers as in the two-layer run-down experiments (Turner, 1967). Thus a model has to be capable of resolving motions on the molecular scales within the SFI, as well as large convective (turbulent) motions. In the oceans the Reynolds and Rayleigh numbers within the convective layers are likely to be large, so that the disparity of scales is considerable. Presently it is beyond the capacity of computers to compute the real-world salt-fingering structures by direct simulation of the Navier Stokes' equations. Piacsek and Toomre (1980) did simulate directly two-dimensional salt fingers. They showed that such salt fingers naturally occur if otherwise linear gradients of salt and temperature are perturbed. They were, however, unable to provide suitable boundary conditions to maintain the salt-fingering structure in a statistically steady state.

Lumley (1980) suggested that a second-order model, if suitably modified, should be able to simulate the statistical properties of the SFI-convective layer system. He argued that the salt fingering can be viewed as a stochastic process with the prevailing motions in the vertical direction. Since the second-order technique proved to be successful in simulating convectively mixed layers (Zeman and Lumley, 1976, 1979; Lumley *et al.*, 1978) one should hope to model the average fluxes, variances and mean profiles of heat and salt if the model equations are made to behave properly in the limit of one-dimensional (1D) motion. This paper reports on the progress in developing such a model. We do not intend here to make a fundamental contribution to the understanding of SFI-convective layer systems; we feel that these systems are already in most respects well understood. Rather, we wish to present a flexible, realistic, inexpensive computational model for such systems. Preliminary results presented in Sections 4, 5 show that the behavior of these systems is realistically predicted. The following two sections deal with development of the model.

2. Salt fingers as a one-dimensional stochastic motion

Ordinary turbulence as found in nature is typically very nearly isotropic in the sense that the departure of the turbulent stress tensor $\overline{u_i u_j}$ from its isotropic value $1/3\overline{q^2}\delta_{ij}$ is small (the quantity $\overline{q^2}$ is twice the kinetic energy of the fluctuating motion). The degree of anisotropy is measured by the nondimensional quantity $b_{ij} = \overline{u_i u_j}/\overline{q^2} - 1/3\delta_{ij}$. Inertial effects in fully developed large Reynolds number turbulence (far enough from the solid boundaries) do not allow $| b_{ij} |_{\max}$ to exceed 0.15 or so, even if buoyancy forces are not negligible. Most second-order models perform well in this range. The smallness of b_{ij} is a convenient property since the modeled terms that are functionals of b_{ij} can be truncated at first order. It turns out, that in rare situations when turbulence becomes very anisotropic, the usual second-

order model equations yield unphysical results (Zeman and Lumley, 1979). If, however, the model equations are made to satisfy the so-called realizability conditions, the unphysical behavior (nonrealizability) can be removed (Schumann, 1977; Lumley, 1979).

One can consider the motion in an SFI as one of the extreme limits of three-dimensional turbulence. The motion is organized in the vertical direction but otherwise it is likely to be random in space and time. In the ocean the Reynolds number in an SFI is not necessarily small, while in the adjacent convective layers it is definitely large. The Rayleigh numbers (in the notation of Turner, 1974)

$$R_s = g\beta\Delta S h^3/\kappa_\theta \nu$$

$$R_\alpha = g\alpha\Delta\Theta h^3 \kappa_\theta \nu$$

(corresponding to an SFI of thickness h and concentration and temperature differences ΔS and $\Delta\Theta$ across the layer) are expected to be much larger than one. Overall, the SFI with the adjacent convective layers can be viewed as a stochastic process where within the SFI the motion tends to the one-dimensional limit and in the adjacent convective layers it is fully turbulent. Our task then, is to form conservation equations for the variances and covariances of the variables involved in the process which satisfy the realizability conditions in the 1D limit, as well as in various other limits associated with small Reynolds and Peclet numbers. Such a (realizable) set should be capable of simulating ensemble-averaged second-order moments in salt-fingering structures.

a. Second moment conservation equations. The second moment (one point) equations which statistically describe the salt-finger process are derived from the governing equations of motion involving two (nonpassive) scalars, salt and temperature. In the Boussinesq approximation, we obtain the following set of (otherwise exact) equations applicable to the horizontally homogeneous field in the mean (Turner, 1974; Lumley, 1980):

$$\dot{\overline{u_1^2}} = \underset{\Pi_{11}}{-2\overline{p_{,1}u_1}/\rho_0} - (\overline{u_1^2 w})_{,z} \underset{2\epsilon_{11}}{-2\nu\overline{u_{1,j}u_{1,j}}}$$

$$\dot{\overline{u_3^2}} \equiv \dot{\overline{w^2}} = 2g(\alpha\overline{\theta w} - \beta\overline{sw}) \underset{\Pi_{33}}{-2\overline{p_{,z}w}/\rho_0} - (\overline{w^3})_{,z} \underset{2\epsilon_{33}}{-2\nu\overline{w_{,j}w_{,j}}}$$

$$\dot{\overline{\theta w}} = -\overline{w^2}\Theta_{,z} + g(\alpha\overline{\theta^2} - \beta\overline{s\theta}) \underset{\Pi_{3\theta}}{-\overline{p_{,z}\theta}/\rho_0} - (\overline{\theta w^2})_{,z} \underset{\epsilon_{3\theta}}{-(\nu + \kappa_\theta)\overline{\theta_{,j}w_{,j}}}$$

$$\dot{\overline{sw}} = -\overline{w^2}S_{,z} + g(\alpha\overline{s\theta} - \beta\overline{s^2}) \underset{\Pi_{3s}}{-\overline{p_{,z}s}/\rho_0} - (\overline{sw^2})_{,z} \underset{\epsilon_{3s}}{-(\nu + \kappa_s)\overline{s_{,j}w_{,j}}}$$

$$\dot{\overline{\theta^2}} = -2\overline{\theta w}\,\Theta_{,z} - (\overline{\theta^2 w})_{,z} - 2\kappa_\theta \overline{\theta_{,j}\theta_{,j}}\}\epsilon_\theta ,$$

$$\dot{\overline{s^2}} = -2\overline{sw}\,S_{,z} - (\overline{s^2 w})_{,z} - 2\kappa_s \overline{s_{,j}s_{,j}}\}\epsilon_s ,$$

$$\dot{\overline{s\theta}} = -\overline{\theta w}\,S_{,z} - \overline{sw}\Theta_{,z} - (\overline{s\theta w})_{,z} - \underbrace{(\kappa_\theta + \kappa_s)\overline{s_{,j}\theta_{,j}}}_{\epsilon_{s\theta}} . \tag{1}$$

$$\dot{\Theta} = -(\overline{\theta w})_{,z}; \quad \dot{S} = -(\overline{sw})_{,z} . \tag{2}$$

Here the vertical axis $x_3 \equiv z$ is oriented upwards, Θ, S are mean temperature and salt concentration, small letters indicate fluctuating parts with zero mean; $\overline{u_3^2} \equiv \overline{w^2}$ is the vertical velocity variance, $\overline{\theta w}$, $\overline{sw}$ are total vertical fluxes of temperature and salt; i.e., in the limit of molecular motion these are respectively $-\kappa_\theta \Theta_{,z}$ and $-\kappa_s S_{,z}$. Since the stochastic motion is axisymmetric with respect to the x_3 axis, the horizontal variances $\overline{u_1^2}$, $\overline{u_2^2}$ are equal. The equations in (1) contain unknown quantities. These are transport terms involving the third-order moments, pressure terms (labeled Π) which are correlations of pressure gradients with other quantities, and molecular terms (labeled ϵ) which are the destruction rates of correlations by molecular smearing; in particular, ϵ is the dissipation rate of the kinetic energy $\overline{q^2}/2$; ϵ_θ, ϵ_s and $\overline{\epsilon_{s\theta}}$ are respectively destruction rates of the temperature variance $\overline{\theta^2}$, the salinity variance $\overline{s^2}$ and the covariance $\overline{s\theta}$. The molecular transport terms involving the gradients of variances are either negligible (on account of large Reynolds numbers) or unimportant. These terms were deleted from (1) and formally absorbed in the third moment terms. Once the unknown terms in (1) are established along with the appropriate boundary and initial conditions the set of equations (1) and (2) can be solved. Our principal objective is to determine the constitutive relationships between the principal variables, the scalar fluxes $\overline{\theta w}$, $\overline{sw}$, and the respective gradients in mean quantities $\Theta_{,z}$, $S_{,z}$. The remaining variables in (1) are not presently accessible to measurements and in that sense they are of secondary importance.

b. Governing equations in the one-dimensional limit. Lumley (1980) suggested that since the motion within the core of the SFI is one-dimensional, the correlation between the fluctuating θ, s and w should be nearly perfect just as in linear stability problems. This does not contradict Stern (1968), who showed that the correlation coefficient of the θ and s *gradients* was not likely to be large. Typical θ and s profiles in an SFI give a correlation coefficient for θ and s of roughly 0.9, while that for the gradients can easily be of order 0.2. Of course, as the correlation coefficient between θ and s increases to 1.0, that between the gradients must also. Furthermore in strictly one-dimensional motion the terms involving gradients with respect to the

axis of the motion must vanish. Hence the set of equations (1) reduce to (Lumley, 1980)

$$
\begin{aligned}
\dot{\overline{w^2}} &= 2g(\alpha\overline{\theta w} - \beta\overline{sw}) - 2\epsilon \\
\dot{\overline{\theta w}} &= -\overline{w^2}\,\Theta_{,z} + g(\alpha\overline{\theta^2} - \beta\overline{s\theta}) - (1 + \kappa_\theta/\nu)\overline{\theta w}/\tau\,, \\
\dot{\overline{sw}} &= -\overline{w^2}\,S_{,z} + g(\alpha\overline{s\theta} - \beta\overline{s^2}) - (1 + \kappa_s/\nu)\overline{sw}/\tau\,, \\
\dot{\overline{\theta^2}} &= -2\overline{\theta w}\,\Theta_{,z} - 2(\kappa_\theta/\nu)\overline{\theta^2}/\tau\,, \\
\dot{\overline{s^2}} &= -2\overline{sw}\,S_{,z} - 2[(\kappa_s/\nu)]\overline{s^2}/\tau\,, \\
\dot{\overline{s\theta}} &= -\overline{\theta w}\,S_{,z} - \overline{sw}\,\Theta_{,z} - [(\kappa_\theta + \kappa_s)/\nu]\overline{s\theta}/\tau\,.
\end{aligned}
\tag{3}
$$

Here, $\epsilon = \nu\overline{(w_{,j}w_{,j})}$, $j = 1,2$, and $\tau = \overline{q^2}/\epsilon$ is the dissipative time scale. For $\epsilon_{3\theta}$, ϵ_{3s}, ϵ_θ, ϵ_s and $\epsilon_{s\theta}$ we used the perfect correlation assumptions (Lumley, 1980)

$$
\overline{\theta_{,j}w_{,j}} = (\epsilon/\nu)\,(\overline{\theta^2}/\overline{w^2})^{1/2},\ \overline{\theta_{,j}\theta_{,j}} = (\epsilon/\nu)\,\overline{\theta^2}/\overline{w^2}\ (j = 1,2)\,,
$$

and similar relations when θ is replaced by s. With the assumption of stationarity Lumley (1980) showed (3) to be reducible to the criterion for salt fingering obtained from the linear stability theory (Turner, 1974)

$$
(\beta S_{,z}/\kappa_s - \alpha\Theta_{,z}/\kappa_\theta)\,(g/\nu)\,(\overline{w^2}/\overline{w_{,j}w_{,j}})^2 \geqslant 1.0\ , \tag{4}
$$

where κ_θ/κ_s, the ratio of heat to salt diffusivities, is about 100.

The assumption of perfect correlation would introduce a numerical error in the critical Rayleigh number applied to real salt fingers, since (as disussed above) the gradients there are not perfectly correlated. The error need not concern us, however, since we do not use this criterion in the development of our model. Our purpose in deriving it here is simply to show that the second moment equations contain the linear stability theory, if taken to the one-dimensional limit.

The development of the models for the various unknown terms in Eq. (1) can be found in Zeman and Lumley (1981, 1982). These models are extensions of the models used for convective turbulence to assure proper behavior in the one- and two-dimensional limits and the limit of perfect correlation. The modeled flow, of course, goes toward these limits, but does not arrive there. All that need concern the oceanographically oriented reader is the recognition that the basic model has been thoroughly explored and is known to work well in convective situations, and that the modifications necessary to include the salt-fingering region follow directly

from the simple physical ideas presented. The reader interested in turbulence modeling will find some points of interest in the way in which this modification is carried out.

3. Scaling of salt-fingering processes

It is expected that at large enough Rayleigh numbers, R_a, and R_s, *the* salt-fingering structure will evolve into a self-similar, statistically steady state and it will be convenient to present the numerical results in a normalized form. The appropriate similarity parameters are not, however, obvious if, in particular, the molecular properties are taken into account. We need to define four fundamental scaling quantities: w_*, Θ_*, S_* the characteristic scales of velocity, temperature and salinity fluctuations within the SFI, and the length scale d associated with the SFI (the spacing of salt fingers). It is apparent that Θ_*, S_* are proportional to $\Delta\Theta$, ΔS the differences across the SFI, where $\Theta_{,z} \cong \Delta\Theta/h$ and $S_{,z} \cong \Delta S/h$ (h is the SFI depth).

In order to estimate w_* let us consider a tube-like flow of diameter d. The descending element of fluid of thickness ΔZ retains its excess density due to the salinity excess ΔS and is acted upon by the downward force

$$(1/4)\pi d^2 \Delta Z \rho_0 \beta \Delta S .$$

This force is counteracted by the frictional force $\pi d \Delta Z \tau_0$, where τ_0 is the shear stress between the finger and adjacent fluid—clearly $\tau_0 = \nu w_*/d$. Equating the driving and the frictional forces we obtain, apart from the unknown proportionality constants

$$w_* = g\beta\Delta d^2/4\nu . \tag{5}$$

The above equation coincides with Turner's (1979) equation (8.3.14) if in his equation the flux ratio $r = \alpha\overline{\theta w}/\beta\overline{sw}$ is set at 1/2. Turner obtained w_* by considering linearized equations for w, θ, s with prescribed square-shaped planforms of salt fingers. Substituting in (5) for d from Turner (1974, 1979) we finally have

$$w_* = (1/2)hN_\theta/R\sqrt{P_r} \tag{6}$$

where $R = \alpha\Delta\Theta/\beta\Delta S$ is the salt finger stability parameter. Hence, for a given temperature gradient $\Delta\Theta/h$, w_* is linearly proportional to the SFI depth and as expected decreases with the stability ratio. Concerning Θ, S_* it is clear that we can safely set $S_* = \Delta S$ because salt is virtually nondiffusive and within the SFI, fluid elements retain their salt concentration. The analogous relationship $\Theta_* \propto \Delta\Theta$ still holds, although $\Theta_* \propto (\overline{\theta^2})^{1/2}$ is likely to be small compared with $\Delta\Theta$ because $\kappa_\theta \gg \kappa_s$.

As suggested by Turner (1967) the salt flux $\overline{sw}$ is related to ΔS by the free convection relationship

$$\beta\overline{sw} \propto (g\kappa_s^2/\nu)^{1/3}(\beta\Delta S)^{4/3} .$$

Linden (1973) and Stern (1976) pointed out that the salt diffusivity κ_s is not the appropriate parameter and as verified later (Schmitt, 1979a; Griffiths and Ruddick, 1980) a more correct scaling law is

$$\beta\overline{sw}_* = A(g\kappa_\theta)^{1/3}(\beta\Delta S)^{4/3}\,, \tag{7}$$

with the coefficient of proportionality $A(R)$ being on the order of 10^{-1} and decreasing with the stability ratio R. We note that with (7) the velocity scale w_* is proportional to $(\beta\Delta S)^{1/3}$ and the length scale $d \propto (\beta\Delta S)^{-1/3}$ (Turner, 1979).

An important parameter and indicator of salt fingering is the density flux ratio $r = \alpha\overline{\theta w}/\beta\overline{sw}$. Both $\overline{\theta w}$ and $\overline{sw}$ are negative (downward) and it is the salt flux which contributes to the kinetic energy production while the heat flux destroys it (see Eq. (1)). Hence, the condition for the existence of salt fingers is $r < 1$. We shall discuss this parameter in detail in the next section.

Within the convective layers the velocity scale is expected to be different from w_*. In analogy with the buoyancy-driven mixed layers we define the convective scale:

$$w_c = (-g\overline{\rho w}h_c/\rho_0)^{1/3}$$

where h_c is the convective layer depth and $\overline{\rho w} = \rho_0\beta\overline{sw}(1-r)$ is the net density flux at the interface between the convective and salt-finger layers. With (7) and $r = \text{const} < 1$ we obtain

$$w_c \propto h_c^{1/3}(\beta\Delta S)^{4/9}$$

and the velocity scale ratio w_c/w_* is

$$w_c/w_* \propto (h_c/h)^{1/3}P_r^{1/9}\,R_s^{1/9}\,. \tag{8}$$

Thus the intensity of convective turbulence depends on the salinity Rayleigh number, which is guaranteed to be large in nature, and on the depth h_c. It is not obvious whether the ratio h_c/h is controlled by the salt-fingering process or whether it depends on the initial (undisturbed) structure of Θ and S. To obtain actual numbers let us use the ocean data of Tait and Howe (1971):

$$h = 7\text{ m},\ h_c \cong 20\text{ m},\ \Delta S \cong 0.03‰ \text{ and } \Delta\Theta = 0.02°\text{C}\,.$$

This gives $R_s = 3.6 \times 10^{11}$ and $w_c/w_* = 35$. Also by (7) we have $w_* = 0.03$ cms^{-1} and $w_c = 1$ cms^{-1}. These are reasonable numbers although the SFI depth $h = 7$ m in the Tait-Howe observations is rather large; perhaps due to vertical distortions of the SFI by waves, currents or even by the induced convection in the adjacent layers. Williams' (1975) observations suggest much smaller h, on the order of centimeters.

4. Simulation of one-dimensional SFI

Observations suggest that within the core of the SFI the motions are very nearly

one-dimensional and it is therefore sensible to first simulate a strictly one-dimensional SFI. From the discussion in 2b, it is evident that this should give essentially the linear stability result. The set of model equations is then greatly simplified: the mean gradients $\Theta_{,z}$, $S_{,z}$ are kept constant and the third-order terms set in (1) are neglected. With the appropriate closure relations (Zeman and Lumley, 1981, 1982) the equations in (1) can be integrated in time. The major purpose of this simulation was to verify the internal consistency of the model, to determine the model free coefficients by comparison with experimental data, and to demonstrate that the model will evolve into a salt-fingering regime regardless of the nature of the initial (perturbation) conditions.

The background conditions were specified by fixing the temperature gradient $\Theta_{,z}$ and the stability parameter $R = \alpha\Theta_{,z}/\beta S_{,z}$. Initially a small isotropy perturbation $q^2{}_0 = 3w^2{}_0/(1 + 3b_{33})$ was introduced with a varying level of anisotropy (in the range between an isotropic (3D) perturbation $b_{33} = 0$ and a 1D perturbation $b_{33} = 2/3$). The initial value of the time scale $\tau = \overline{q^2}/\epsilon$ was determined by the thermal Brunt-Väisälä frequency N_θ, i.e.:

$$\tau N_\theta \cong 1.0 \ .$$

The initial energy level $\overline{q^2}_0$ was set by the condition that the initial (total) viscosity is essentially molecular so that the Reynolds number $R_c = (\tau\overline{w^2}/2\nu)_0$ is on the order of unity. Initial conditions for the remaining variables in (1) turned out to be unimportant as long as the decay scales τ_θ and τ_s were of the same order as, or larger than, τ. The molecular properties were specified as follows: for the heat-salt case $P_r = \nu/\kappa_\theta = 7$ and the diffusivity ratio $\sigma = \kappa_\theta/\kappa_s = 100$; for the salt-sugar case $P_r = 700$ and $\sigma = 3$. The water kinematic viscosity was taken to be $\nu = 0.0135$ cm^{2}s^{-1}.

The one-dimensional salt-fingering process is unsteady—the model equations are linear and kinetic energy grows exponentially. There is, however, a self-similar asymptotic state in the sense that all quantities grow in proportion to each other; in particular, the flux ratio r asymptotes to a constant value independent of the initial condition. Needless to say, all the variables attain the exact 1D limit as revealed by correlation coefficients and time scale ratios, and demanded by Eq. (3). Thus the important property of the model is that regardless of the details of the initial perturbations, the model gravitates toward the salt-fingering state if the background stratifications of salt and temperature are favorable.

Figure 1 shows the fundamental results of the predicted dependence r vs. R for two cases known in the literature; the heat-salt case in Figure 1a and the salt-sugar case in Figure 1b. It turned out that the calculated r was sensitive only to the value of a constant associated with the Brunt-Väisälä term in the dissipation equation. The value for the heat-salt case was chosen to match the Turner (1967) average experimental value of $r = 0.56$ for $R > 2.0$. The functional dependence of this con-

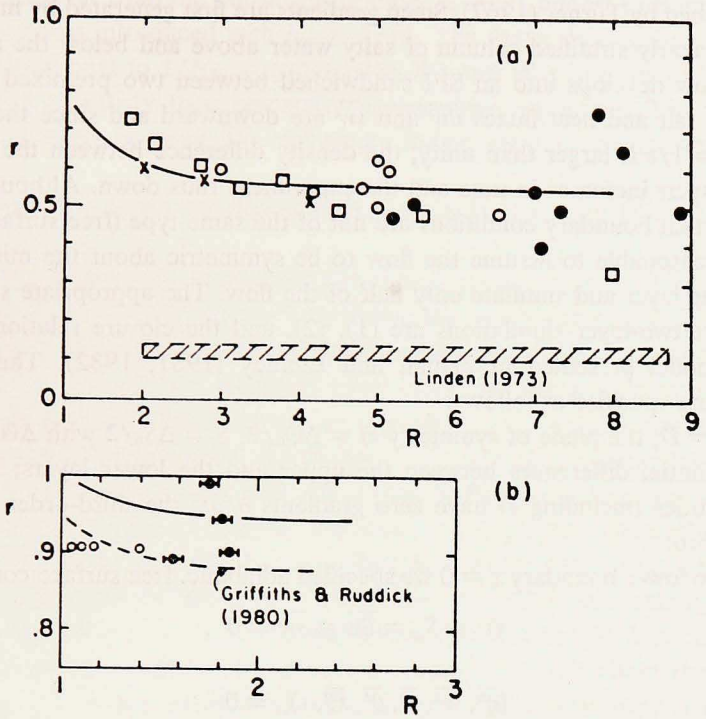

Figure 1. Comparison with data of the computed flux ratio r as a function of the stability parameter $R = \alpha\Theta_{,z}/\beta S_{,z}$. Solid curves are 1D model calculations; (a) heat-salt case: ○, ●, X are data points of Turner (1967); □ Schmitt (1979b); (b) salt-sugar case: ○, Stern and Turner (1969); ●, Lambert and Demenkow (1972).

stant on P_r suggested in Zeman and Lumley (1981, 1982) is only tentative; it was needed to obtain reasonable values of the flux ratio for the salt-sugar case. It is worth noting that recent salt-finger results of Schmitt (1979b) also shown in Figure 1a were obtained without external stirring of the adjacent, convective layers. Stirring was employed by Turner (1967) and Linden (1973). Schmitt's data show a continued decreasing trend with R, while Turner's data level off for $R > 2$.

In real-world salt-fingering structures, one-dimensional motions are possible only in the core of the SFI. The excess of the kinetic energy generated in the core is likely to be exported toward the edges of the SFI where the energy can be more efficiently dissipated by interactions with the convective turbulence. This export of $\overline{q^2}$ can be effected only through the transport terms $\overline{q^2 w}$. The export mechanism is evident in the two-layer simulations presented in the next section.

5. Simulation of the two-layer experiment

The simplest autonomous salt-fingering flow is the two-layer run-down experi-

ment described by Turner (1967). Steep gradients are first generated by mechanically stirring a linearly stratified column of salty water above and below the mid-height. Thus the flow develops into an SFI sandwiched between two premixed convective layers. The salt and heat fluxes $\overline{\theta w}$ and $\overline{sw}$ are downward and since the flux ratio $\beta\overline{sw}/\alpha\overline{\theta w} = 1/r$ is larger than unity, the density difference between the upper and the lower layers increases in time and the experiment runs down. Although the true top and bottom boundary conditions are not of the same type (free surface vs. solid wall) it is reasonable to assume the flow to be symmetric about the middle of the salt-fingering layer and simulate only half of the flow. The appropriate set of equations for the two-layer simulations are (1), (2), and the closure relations, and the transport model presented in Zeman and Lumley (1981, 1982). The boundary conditions are specified as follows:

(a) at $z = D$, the plane of symmetry $\Theta = \Delta\Theta_0/2$, $S = \Delta S_0/2$ with $\Delta\Theta$, ΔS_0 being prescribed initial differences between the upper and the lower layers; all second-order quantities (including ϵ) have zero gradients $\partial/\partial z$, the third-order (transport) terms are zero;

(b) at the lower boundary $z = 0$ we specified adiabatic, free surface conditions

$$\Theta_{,z} = S_{,z} = \overline{\theta w} = \overline{sw} = 0 \ ,$$

and

$$(\overline{q^2}, \overline{w^2}, \overline{s^2}, \overline{\theta^2}, \overline{s\theta}, \epsilon)_{,z} = 0 \ .$$

Setting up appropriate initial conditions caused some difficulty. We were unable to satisfactorily simulate the mechanism of stirring employed in the Turner experiment. Rather we assumed that both temperature and salt were already premixed so that they were constant throughout the bottom layer with steep gradients in S and Θ near $z = D$. For convenience we chose the following functions

$$\Theta(z) = (\Delta\Theta_0/2)\exp\{2(z/h_0 - D/h_0)\}$$

$$S(z) = \Theta(z)\Delta S_0/\Delta\theta_0 \ ,$$

where h_0 is the depth of the steep-gradient region. Hence $\Delta\Theta_0$, ΔS_0 and h_0 define the scaling parameters of the problem. The initial stability ratio $R_0 = \alpha\Theta_0/\beta\Delta S_0$ was usually set at 1.5 to 2; values smaller than 1.5 resulted in intense mixing and a rapid decay of the SFI. Similar problems were encountered in the actual experiment (Turner, 1967). The depth h_0 was typically on the order of centimeters and the maximum gradient $\Theta_{,z}(z = D) = \Delta\Theta_0/h_0$ was limited by numerical stability to values below 0.01°C/cm. The coefficients in the transport model were given values similar to those in Zeman and Lumley (1976, 1979). Although the results are not sensitive to changes in the constants within 20% or so, the transport terms are indispensable for maintaining convective turbulence.

As in the previous simulations we deliberately set the initial conditions for the

second moments far from the salt-fingering state. A small, almost isotropic perturbation $\overline{q^2} = w_{*_0}{}^2$ was introduced with $b_{33} = 1/15$. The decay time scales $\tau = \tau_\theta = \tau_s$ were set proportional to $1/N_{\theta_0} = (\alpha\Delta\Theta_0/\beta\Delta S_0)^{1/2}$ and all other quantities were set approximately to satisfy their respective conservation equations. The initial field represents, in effect, a weak 3D turbulence independent of molecular properties of the fluid.

Unless otherwise noted we simulated the salt-heat case with $P_r = 7$, $\sigma = 100$ and $h_0/D = 0.1$.

To simulate mechanical stirring we introduced virtual sources of kinetic energy through virtual fluxes $\overline{q^2 w}$ placed in-between the neighboring grid levels. These fluxes were Gaussian distributed around the mid-height of the convective layer and on the order of $w_{*_0}{}^3$. As the numerical experiment was running down due to ever-increasing stability the virtual fluxes were switched on for a short time to stimulate the convective turbulence without disturbing the formed salt-fingering layer.

Typical results of the simulations are shown in Figures 2 through 6 where the lower half of a two-layer (symmetric) experiment is displayed. The evolution of the anisotropy coefficient b_{33} in Figure 2 best illustrates the formation of salt fingers. The numbers on each curve designate time in multiples of the SFI time scale $\tau_{sf} = h_0/w_{*_0}$. We observe that after about $t = 6\tau_{sf}$ the initial, almost isotropic, layer evolves into two distinct regions: a thin layer (symmetric about $z = D$) where the motion is vertical ($b_{33} = 2/3$) and the deep underlying layer where anisotropy is fairly small and corresponds to typical convective turbulence ($b_{33} = 1/6$). The thin 1D layer has all the attributes of the salt-fingering process: the flux ratio r is smaller than unity (typically 0.5-0.6), the salt flux $\overline{sw}$ is convective and scales on $(\overline{sw})_*$ with the constant $A_0 = \beta\overline{sw}/(g\kappa_\theta)^{1/3}(\beta\Delta S_0)^{4/3} = 0.28\text{-}0.05$. Schmitt (1979b) observed A in the range 0.04 to 0.16, decreasing with stability. The erratic behavior of $\overline{sw}$ in the vicinity of the SFI shown in Figure 3 indicates that the flow is not near equilibrium. Salt, and consequently also heat, are being redistributed as the SFI evolves. Large fluctuations with height of $\overline{sw}$ are caused by a poor match between the prescribed initial profiles of S (and Θ) and those corresponding to the salt-fingering structure. The way S and Θ are redistributed is displayed in Figures 5 and 6. We note that the S profile develops an inflection point just below $z = D$. The gradient $S_{,z}$ tends to decrease within SFI due to the double-diffusive convection; this necessitates a steeper gradient just below the SFI and the inflection point.

Figure 3 shows the development of the kinetic energy $\overline{q^2}$. We note that the profile of $\overline{q^2}$ has recognizable features of a convective structure with the overlying SFI. The convective activity is not as intense as anticipated but this may be due to the absence of a more realistic transport model. As mentioned earlier, off-diagonal terms in the transport coefficient matrix (Zeman and Lumley, 1976) have been neglected in our model. The increase of $\overline{q^2}$ between times $9\tau_{sf}$ and $12\tau_{sf}$ is due to the enhancement

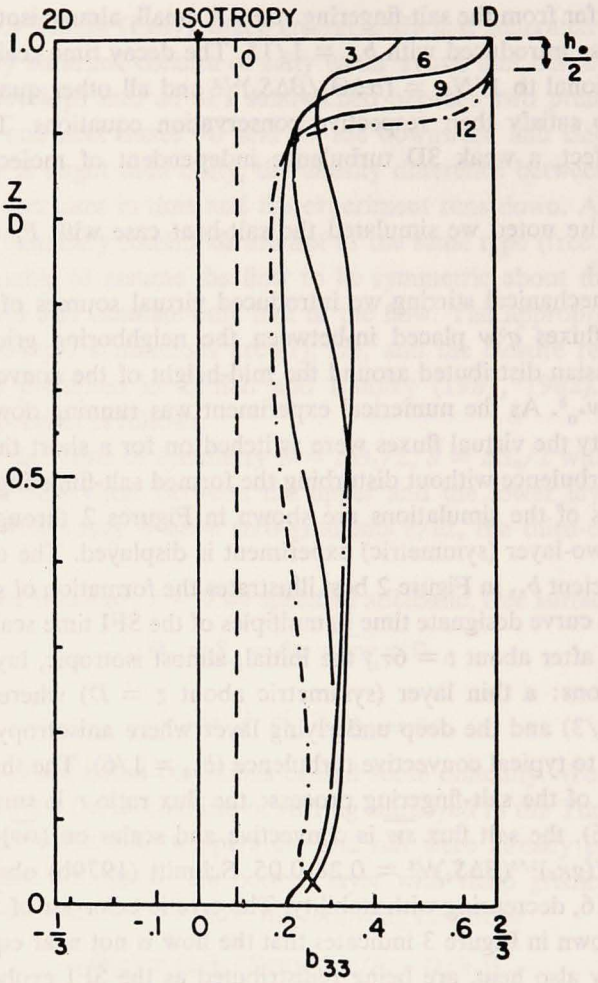

Figure 2. Computed profiles of the anisotropy tensor component $b_{33} = w^2/q^2 - 1/3$ during the evolution of the two layer calculation. Numbers on the profiles mark time in multiples of the SFI time scale $\tau_{sf} = h_0/w_{*0}$.

of convection by "stirring." In the previous section we suggested the so-called export mechanism: the need to export the excessive energy produced by the salt-finger convection away from the SFI core. The local maximum of $\overline{q^2}$ at $z = D$ indicates that this mechanism is at work.

6. Conclusions

Although our ultimate goal is to apply the present model to oceanic multilayer flow structures, it was a necessary step to test the model on this simple two-layer experiment. The fact that the model is capable of maintaining a quasi-equilibrium

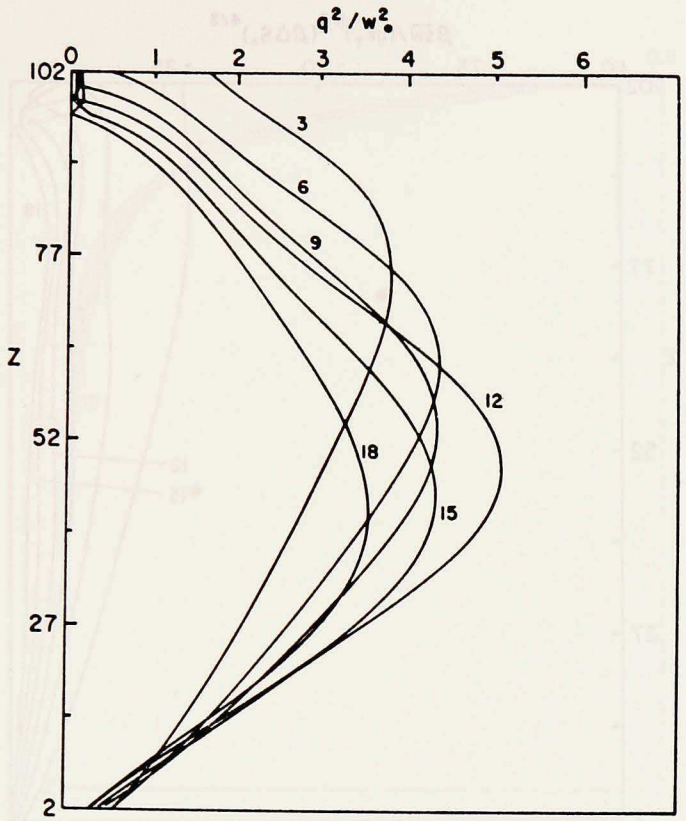

Figure 3. Computed profiles of the kinetic energy q^2. The scale q^2/w_{*0}^2 is shown on the top; same as Figure 2.

salt-fingering process not constrained by unphysical boundary conditions or by small amplitude (linear) assumptions is, we feel, a major step in the direction of modeling the real-world oceanic salt fingers. The model contains the physical mechanisms that are essential to forming a salt-fingering regime.

As concerns future work it is desirable to determine experimentally the actual Reynolds number dependence of the return-to-isotropy function. The presently used transition function (Zeman and Lumley, 1981, 1982) reflects experimental evidence that mechanisms characteristic for large *Re* turbulence arise suddenly (Chung and Adrian, 1979). Conceivably this effect has to do with the criticality of the Reynolds number. An analogy may be drawn between the viscous sublayer (in a turbulent boundary layer) and the salt-fingering interface. The buffer zone may be likened to the salt-finger-convective interface. The various functions that we use to switch off and on the 1D or 3D modes (Zeman and Lumley, 1981, 1982) are not important for the SFI itself; however, they do affect the buffer zone between the salt fingering

Figure 4. Computed profiles of the salt flux $\overline{sw}$; same as in Figure 2.

and convective layers. Not presently accessible to measurements, these functions may have to be inferred from direct numerical simulations of the Navier-Stokes' equations.

Acknowledgments. This work was supported in part by the U.S. Office of Naval Research under the following programs: Physical Oceanography (Code 481); Power (Code 473); and Fluid Dynamics (Code 438); and by the U.S. National Science Foundation, Division of Atmospheric Sciences, under Grant No. ATM 79-22006. We wish also to acknowledge the invaluable help of Gene Terray in connection with programming.

REFERENCES

Chung, M. K. and R. J. Adrian. 1979. Evaluation of variable coefficients in second order turbulence models, *in* Proc. Turbulent Shear Fow Symposium, London, 1043–1048.

Griffiths, R. W. and B. R. Ruddick. 1980. Accurate fluxes across a salt-sugar finger interface deduced from direct density measurements. J. Fluid Mech., *99*, 85–95.

Kerr, R. A. 1981. Fingers of salt help mix the sea. Science, *211*, 155–157.

Lambert, R. B. and J. W. Demenkow. 1972. On the vertical transport due to fingers in double diffusive convection. J. Fluid Mech., *54*, 627–640.

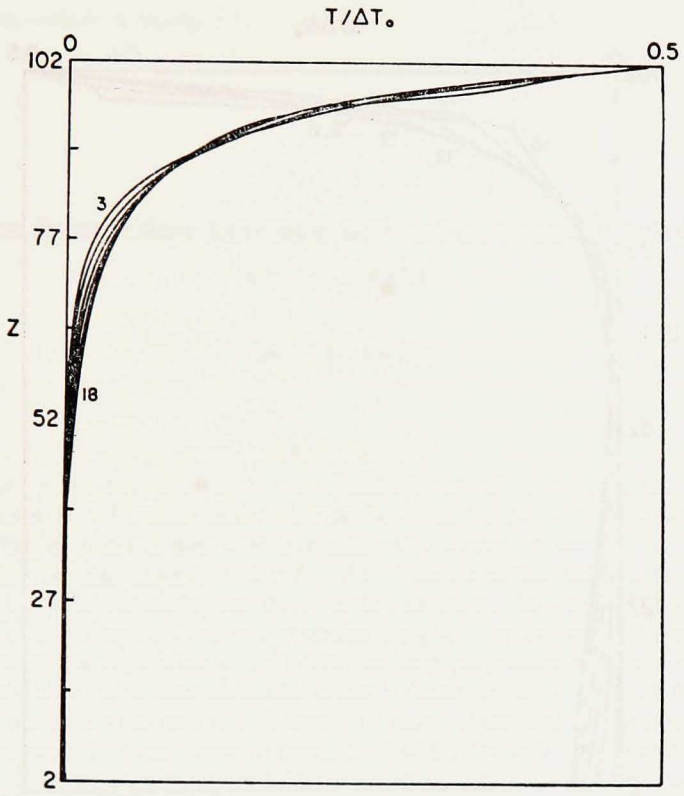

Figure 5. Computed profiles of the mean temperature Θ; same is in Figure 2.

Linden, P. F. 1973. On the structure of salt fingers. Deep-Sea Res., *20*, 325–340.

Lumley, J. L. 1979. Computational modeling of turbulent flows. Appl. Mech., *18*, 123–176.

—— 1980. Some fundamental aspects of turbulence with implications in geophysical flows, *in* Marine Turbulence, J. C. J. Nihoul, ed., Elesvier Amsterdam, 175–192.

Lumley, J. L., O. Zeman and J. Siess. 1978. The influence of buoyancy on turbulent transport. J. Fluid Mech., *84*, 581–597.

Piacsek, S. A. and J. Toomre. 1980. Nonlinear evolution and structure of salt fingers, *in* Marine Turbulence, J. C. C. Nihoul, ed., Elsevier Amsterdam, 36–63.

Schmitt, R. W. 1979a. The growth rate of supercritical salt fingers. Deep-Sea Res., *26*A, 23–40.

—— 1979b. Flux measurements of salt fingers at an interface. J. Mar. Res., *37*, 419–436.

Schumann, U. 1977. Realizability of Reynolds stress turbulence models. Phys. of Fluids, *20*, 721–725.

Sherman, F. S., J. Imberger and G. M. Corcos. 1978. Turbulence and mixing in stably stratified waters. Ann. Rev. Fluid Mech., *10*, 267–282.

Stern, M. E. 1960. The 'salt fountain' and thermohaline convection. Tellus, *12*, 172–175.

—— 1968. T-S gradients on the micro-scale. Deep-Sea Res., *15*, 245–250.

—— 1976. Maximum buoyancy flux across a salt finger interface. J. Mar. Res., *34*, 95–110.

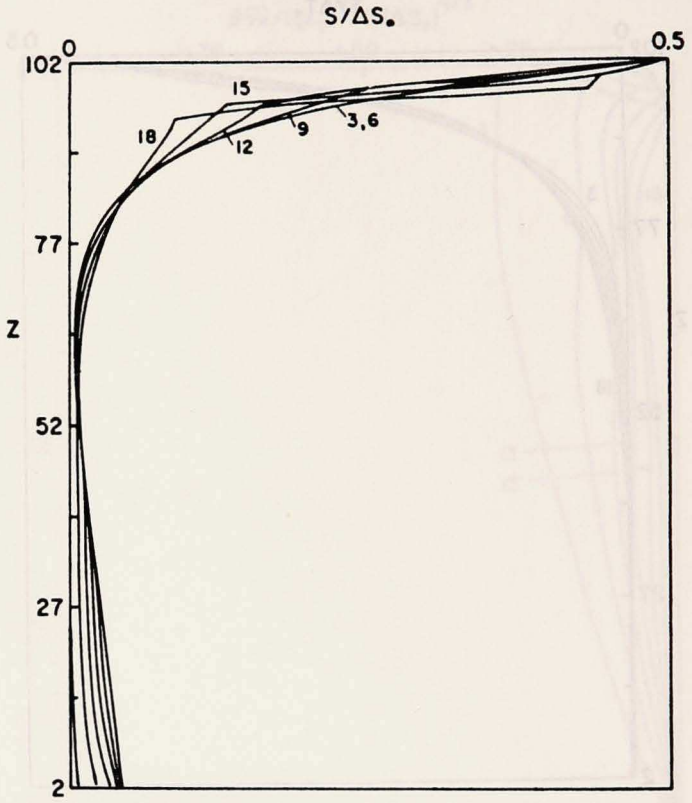

Figure 6. Computed profiles of the mean salt concentration S; same as in Figure 2.

Stern, M. E. and J. S. Turner. 1969. Salt fingering and convective layers. Deep-Sea Res., *16*, 497–511.

Tait, R. I. and M. R. Howe. 1971. Thermocline staircase. Nature, *231*, 178–179.

Turner, J. S. 1967. Salt fingers across a density interface. Deep-Sea Res., *14*, 599–611.

—— 1974. Double-diffusive phenomena. Ann Rev. Fluid Mech., *6*, 37–56.

—— 1979. Buoyancy Effects in Fluids. Cambridge University Press, London.

Williams, A. J. 1975. Images of ocean microstructure. Deep-Sea Res., *22*, 811–829.

Zeman, O. and J. L. Lumley. 1976. Modeling buoyancy driven mixed layers. J. Atmos. Sci., *33*, 1974–1988.

—— 1979. Buoyancy effects in entraining turbulent boundary layers: a second order closure study, *in* Turbulent Shear Flows I, F. Durst, B. E. Launder, F. W. Schmidt and J. H. Whitelaw, eds., Springer-Verlag, Berlin/Heidelberg, 295–302.

—— 1981. Modeling Salt-Fingering Structures. Sibley School of Mechanical and Aerospace Engineering Report No. FDA-81-03, Cornell University, Ithaca, New York.

—— 1982. Progress in modeling multi-layer salt-fingering structures, *in* Applications of Fluid Mechanics and Heat Transfer to Energy and Environmental Problems, D. D. Papailiou and D. K. Papailiou, eds., Springer-Verlag, Berlin/Heidelberg/New York, (in press).

Received: *10 April, 1981*; revised: *11 December, 1981.*